Available online at www.sciencedirect.com
SCIENCE DIRECT®
Journal of Nuclear Materials 335 (2004) 417–424
journal of nuclear materials
www.elsevier.com/locate/jnucmat

Analysis on Lift-Off experiment in Halden reactor by FEMAXI-6 code

M. Suzuki [a,*], K. Kusagaya [b,1], H. Saitou [c], T. Fuketa [a]

[a] Department of Reactor Safety Research, Japan Atomic Energy Research Institute, Tokai-mura, Naka-gun, Ibaraki-ken 319-1195, Japan
[b] JAERI, Tokai-mura, Naka-gun, Ibaraki-ken 319-1195, Japan
[c] CRC Solutions Corp., 2-7-5 Minamisuna, Koto-ku, Tokyo 136-8581, Japan

Received 2 February 2004; accepted 11 July 2004

Abstract

Analysis was conducted on the Lift-Off experiment IFA-610.1 in Halden reactor by the FEMAXI-6 code using detailed measured data in the test-irradiation. Fuel center temperature was calculated on the two assumptions, i.e. (1) an enhanced thermal conductance across the pellet-clad bonding layer is maintained during the cladding creep-out by over-pressurization, and (2) the bonding layer is broken by the cladding creep-out, and these results were compared with the measured data to analyze the effect of the creep-out by over-pressure inside the test pin. The measured center temperature rise was higher by a few tens of K than the prediction performed on the assumption (1), though this difference was much smaller than the predicted rise on the assumption (2). Therefore, it is appropriate to attribute the measured center temperature rise to the decrease of effective thermal conductance by irregular re-location of pellet fragments, etc. which was caused by cladding creep-out.

PACS: 28.50.−k

1. Introduction

In high burnup fuel rods of LWR, fission gas release is capable of being enhanced and internal gas pressure is elevated. If the internal pressure exceeds the coolant pressure to a large extent, cladding begins outward creep and pellet-clad gap, which has been closed, re-opens. This phenomenon has been termed 'Lift-Off'. As a result, fuel temperature rises due to reduced thermal conductance across the gap and the fission gas release is further enhanced, thus augmenting the internal pressure and the gap width again. Fuel rod must avoid this positive feedback in actual cases.

To obtain the threshold over-pressure, i.e. excess pressure of internal gas over coolant pressure to cause the Lift-Off, experiment using irradiated test rod was conducted in Halden as IFA-610.1 test [1]. The test rod was originally a segment of a PWR-type rod which had been base-irradiated up to average burnup of 52 GW d/tUO_2 in a commercial PWR in Switzerland. The segment was re-fabricated into a test rod which was instrumented with center thermocouple and cladding extensometer.

* Corresponding author. Tel.: +81 29 282 5295; fax: +81 29 282 5323.
E-mail address: motoe@popsvr.tokai.jaeri.go.jp (M. Suzuki).
[1] Cooperative staff of JAERI until March 2002.

0022-3115/$ - see front matter © 2004 Elsevier B.V. All rights reserved.
doi:10.1016/j.jnucmat.2004.07.049

In this experiment, the fuel center temperature was measured during over-pressurization by Ar gas which was supplied from the out-reactor source through a pipe, and the threshold over-pressure to cause a significant rise in the temperature was estimated but the cladding diameter change by creep was not measured.

However, it is important for fuel temperature to be evaluated in association with the gap thermal conductance change. Also, it is essential in high burnup fuel analysis to estimate the thermal conductance change by the presence of bonding layer that has been generated by chemical reaction of pellet outer surface and cladding inner surface.

In the present analysis, to elucidate these points, the thermal behavior of IFA-610.1 test rod was investigated by the use of fuel performance code FEMAXI-6 [2], and implications of the experiment were evaluated.

2. Method

2.1. FEMAXI-6 code

The FEMAXI-6 code, which has been developed by the first and the third authors as an advanced version of the former version FEMAXI-V [3,4], performs analysis on the irradiation behavior of LWR fuel in both normal operating and anticipated transient conditions, dealing with thermal and mechanical phenomena and their interactions of a single rod during whole life period. In the FEMAXI-V code, a simplified mechanical calculation was performed in thermal analysis part to determine the gap width and pellet-clad contact pressure independently from the detailed mechanical analysis which was conducted by two-dimensional FEM model for the entire length of fuel rod. The difference between the results of this simple analysis and detailed analysis became out of negligible extent in the high burnup region, giving uncertainty in calculation.

Consequently, in the FEMAXI-6 code, the detailed mechanical analysis and thermal analysis are directly coupled, i.e. result of FEM deformation analysis is given to the calculation of such thermal analysis as gap conductance, etc. and vise versa through the iteration of two predictions, deformation and temperature, at each time step.

2.2. Models and materials properties

Main models and materials properties are listed below.

(1) Fuel thermal conductivity: Halden model which was obtained on the in-pile temperature data [5].
(2) Fuel swelling: Studsvik model proposed by Schrire et al. [6].
(3) Mechanical and thermal properties of pellet and cladding, such as elasticity and thermal expansion: MATPRO-11 models [7].
(4) Gap thermal conductance: RS-gap case using the modified Ross and Stoute model [8], and BD-gap case using the bonding model described below.
(5) Cladding creep: McGrath's model [9], which has been used for analysis and evaluation of in-pile creep experiments of Halden Reactor Project.

2.3. Bonding layer model

A detailed PIE observation on high burnup fuel has revealed that the bonding layer with a typical thickness of 10 μm consists of main part of ZrO_2, some portion of UO_2 and non-stoichiometric zirconia [10]. Therefore, a good approximation can be obtained for the thermal conductance of the bonding layer by assuming that the layer is simply ZrO_2 with 10 μm thickness. Here, this thermal conductance is set as **BDC**. If thermal conductivity of ZrO_2 is adopted from MATPRO-A [11] as

$$k = 0.835 + 1.81 \times 10^{-4} T \quad (\mathrm{W/mK})\ \mathrm{T:\ K}. \tag{1}$$

BDC is around 10 W/cm^2 K, giving more than ten times larger value than 0.2 (open gap) ~1 W/cm^2 K (closed gap) by the Ross–Stoute model in open or closed gap conditions. On these considerations, a bonding model which has been described in Ref. [2] and incorporated in the code is shown here again, since evaluation of bonding gap conductance is essential in the present analysis:

(1) Progress of bonding layer formation, **BD**, between pellet and cladding is defined as

$$BD = \int_{t_{\mathrm{start}}}^{t} P_{\mathrm{c}}\,\mathrm{d}t/X \quad (0 \leqslant BD \leqslant 1.0), \tag{2}$$

where P_c: pellet-clad contact pressure, t_{start}: time of contact start, X: empirical parameter (h MPa).
Eq. (2) is applied during the contact period. When BD reaches unity, bonding layer formation is assumed to be completed. 'X' is tentatively set as 10 000–20 000 in the present analysis. The overall calculation results are not sensitive to the value 'X'.

(2) Gap conductance is defines as:
   (a) The Ross and Stoute model conductance is adopted as long as **BD** = 0, i.e. open gap is maintained.
   (b) When gap is closed and bonding layer formation is in progress, the conductance is **GC2** and it is defined as

$$\mathbf{GC2} = (1 - \mathbf{BD}) \cdot \mathbf{GC1} + \mathbf{BD} \cdot \mathbf{BDC}, \tag{3}$$

where **GC1** is the conductance determined by the Ross–Stoute model in the closed gap condition tak-

ing account of the contact pressure. Thus, when the layer is completed, **BD** = 1 holds and the conductance is equal to **BDC**.

2.4. Gap re-opening after *BD* = 1

In the condition where cladding outward creep begins by over-pressure after **BD** = 1 is attained and the mechanical analysis gives gap 're-opening', the present analysis compared the calculations on the basis of the following two assumed modes concerning the 'gap thermal conductance':

In 'RS-gap case', i.e. 'bonding-to-Ross and Stoute' model, the bonding model conductance **BDC** is applied to the period during which closed gap is predicted, while the Ross and Stoute model conductance **GC1** is applied to the rest period during which the mechanical analysis predicts an open gap.

In 'BD-gap case', once after **BD** = 1 has been attained by the calculation of Eq. (2), **BDC** is applied irrespective of the result of the mechanical analysis prediction, i.e. **BDC** is applied even if gap re-opens numerically in the mechanical analysis which models that the bonding layer does not glue the pellet outer surface to the cladding inner surface but only equalizes the axial displacements of the two surfaces.

2.5. Input data

To minimize the uncertainty of calculation associated with the input data, the measured test conditions were given to the calculation as faithfully and elaborately as possible.

2.5.1. Fuel rod specifications

Main specifications of the PWR type test rod used in the experiment is listed in Table 1 [1].

Since the present analysis covers both the base- and test-irradiation periods in a single continuous calculation, fuel stack length is set throughout the calculation as 422 mm which is the re-fabricated length for Halden reactor test. Initial plenum volume for the base-irradiation period was set as a rough estimate of 1.3 cm^3, which was obtained by multiplying 11 cm^3, a representative value for plenum volume of a full-length PWR rod, with the ratio of stack length 422–3700 mm. Also, in the test-irradiation period, effects of calculated fission gas release and fuel temperature change on the internal gas pressure were reduced to a negligible extent by setting the plenum volume to be virtually very large, i.e. 1000 cm^3. This is evidently justified by the experimental settings in which the external Ar gas was supplied to the test rod through a pipe.

2.5.2. Irradiation history in calculation

The base-irradiation history consists of a simplified power history [1] and coolant condition of the test-irradiation period, i.e. inlet temperature is 583 K, pressure is 15 MPa, and flow rate is 3.35×10^3 $kg/m^2 s$ [1,12]. The fast neutron flux was set as 6.4×10^{13} n/cm^2 s for the whole period so that the fluence calculated in FEMAXI-6 at the end of the base-irradiation reached roughly 8×10^{21} n/cm^2 [1].

The histories of linear power, fast flux, and coolant conditions, i.e. temperature, pressure, and flow rate, during the test-irradiation period were all referred to and derived from the TFDB: Test Fuel Data Bank [12] of Halden Reactor Project. The most essential factors in these data, linear power and fast flux dominating fuel temperature and cladding creep rate, respectively, are shown in Fig. 1.

2.5.3. Axial profile of power

In the calculation, the stack part of the test rod was divided into 6 equal-length axial segments, to each of which a relative weight factor was given to be multiplied by the average linear power. During the base-irradiation, the axial profile of power was assumed to be flat, i.e. the relative values are all unity.

During the test-irradiation, a parabolic curve was fitted to the three values of linear power in the TFDB at the top, middle and bottom elevations of test rod, and this parabolic curve was divided into six axial segments, and at each of the six segments the relative weight factor was derived by averaging the parabolic curve. The axial profile changed with time during the experiment, so that

Table 1
Specifications of the IFA-610.1 test rod [1]

As-fabricated	Pellet	Diameter: 9.12 mm, density: 96.1% TD
	Cladding	Partly re-crystallized Zircaloy-4
		Outer diameter: 10.75 mm, inner diameter: 9.29 mm
		Rod internal pressure 2.15 MPa by He
At the beginning of test-irradiation	Pellet	Average burnup: 52 GW d/tUO_2
		Stack length: 422 mm
		Inner hole diameter for thermocouple: 2.3 mm
	Cladding	Fast neutron fluence: $\sim 8 \times 10^{21}$ n/cm^2 (>1 MeV)
		Outer oxide layer thickness: 40–60 μm, 45 μm at thermocouple elevation

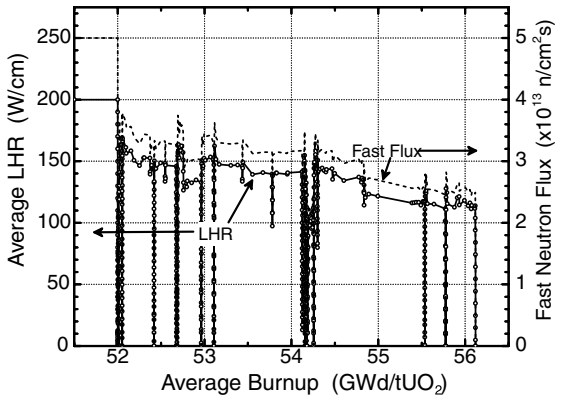

Fig. 1. Average linear heat rate and fast neutron flux adopted in the calculation for the test-irradiation period.

for all the input points consisting the power history, corresponding relative factors for the six segments were specified using the parabolic curve fitting to the TFDB data. The relative axial profiles at some representative burnups are shown in Fig. 2.

A fuel-center thermocouple was inserted in the test rod at 39 mm depth from the top of pellet stack, and the stack penetrated by the thermocouple consisted of hollow pellets with center hole of 2.3 mm diameter. In accordance with this geometry, the calculation set hollow pellets in the top 6th segment. The center elevation of this 6th segment is 35 mm, nearly corresponding to the thermocouple top elevation.

2.5.4. Radial power profile

Burnup-dependent power density profile in the radial direction of pellet was obtained by the burning analysis code RODBURN [13], and the results were given to the

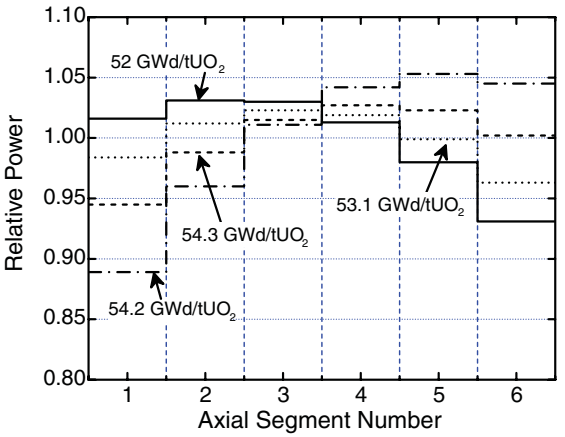

Fig. 2. Relative axial power profiles adopted in the calculation for the six segments of test rod at some representative burnups during the test-irradiation period.

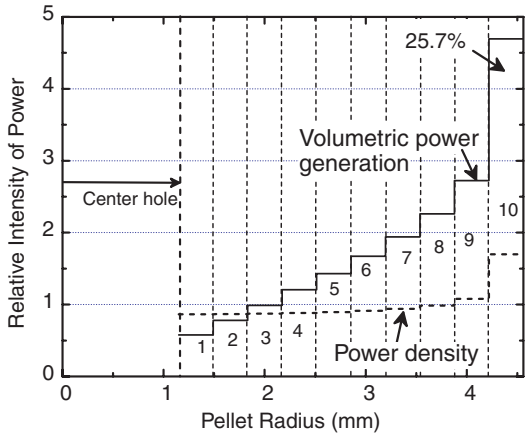

Fig. 3. Relative power generation density and volumetric power generation in the ten radial ring elements of the fuel pellet at the top axial segment. The power density is obtained by RODBURN calculation.

ten concentric equal-thickness ring elements in the radial direction of pellet. In Fig. 3, this relative power density profile at the start of the test-irradiation is shown by broken line and also a relative volumetric power generation is shown by thick line. The latter is referred to in the discussion later.

2.5.5. Cladding waterside oxide layer

Cladding outer surface oxide thickness calculation was conditioned so that the thickness at the thermocouple elevation calculated by FEMAXI-6 may be identical to the measured value (45 μm; Table 1) at the start of the test-irradiation by adjusting the oxide growth rate of the code model.

3. Results

3.1. Over-pressure, cladding creep-out, and gap conductance

The first target of the present analysis is cladding creep-out and its associated 'numerical' increase of pellet-clad gap. The 'numerical' is termed considering the actual case where pellet fragment bonded to the cladding moves with cladding creep-out. Cladding diameter increase by creep with the over-pressure is shown in Fig. 4 during the test irradiation, and the numerical gap is shown in Fig. 5.

These calculated results are obtained with the RS-gap case and BD-gap case described in Section 2.3. In the mechanical analysis of FEMAXI-6, a dragging displacement of bonded pellet fragment in the radial direction induced by cladding creep-out is not modeled even in the period where the thermal calculation through the

bonding layer is performed. Therefore, the numerical gap in Fig. 5 which is brought about by over-pressure is of virtual nature for the bonding gap. In other words, while Figs. 4 and 5 indicate that over-pressure increases cladding diameter and re-opens the gap, it is another matter whether bonding layer breaks and gap re-opens or not in actual situations. However, Fig. 5 can indicate the magnitude of gap re-opening which inevitably occurred in some location of pellet radius. This is one of the important pieces of information given by the present analysis.

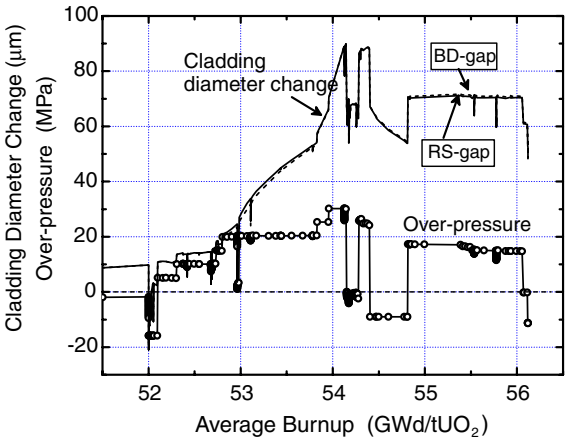

Fig. 4. Measured over-pressure and calculated cladding diameter changes by bonding gap model (BD-gap) and by Ross–Stoute model (RS-gap) at the top axial segment during the test-irradiation period.

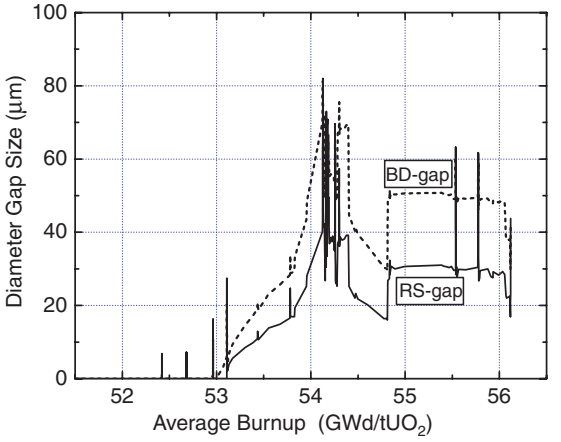

Fig. 5. Gap sizes calculated by bonding gap model (BD-gap) and by Ross–Stoute model (RS-gap), at the top axial segment during the test irradiation period.

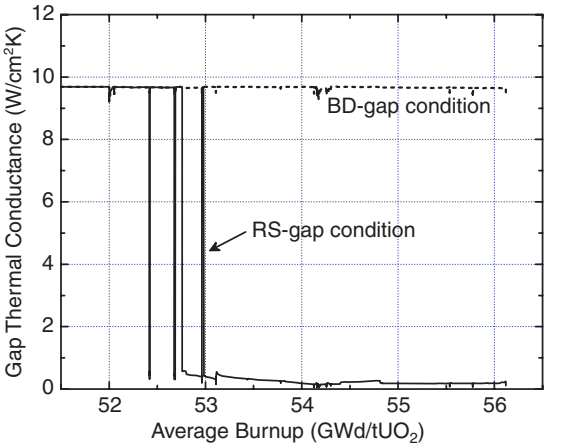

Fig. 6. Gap thermal conductances calculated by two models, bonding gap model (BD-gap) and by Ross–Stoute model (RS-gap), at the top axial segment during the test-irradiation period.

The calculated gap in Fig. 5 is larger in the BD-gap case than that in the other, which is caused mainly by the condition in which pellet thermal expansion is smaller by 20–30 μm due to the temperature fall by enhanced thermal conductance of bonding layer.

Fig. 6 shows the calculated thermal conductances in the RS-gap case and in the BD-gap case. In the RS-gap case, the thermal conductance is given by BDC in the early period, while it is given by the Ross–Stoute model in the period during which gap re-opening is predicted due to the over-pressure and power shut-down, which gives an abrupt change of conductance.

3.2. Fuel center temperature

The calculated fuel center temperatures at the 6th segment during the test-irradiation period by the BD-gap case and RS-gap case are given in Fig. 7 with the measured data for comparison.

(1) RS-gap case result (thick line): The original numerical prediction resulted in a higher temperature than the measurement by 15 K in the preparatory period (up to 52.0 GW d/t) of the test-irradiation with no over-pressure. This over-estimate is attributable to a combination of various factors such as measurement errors, numerical model inaccuracy, etc. Here, to focus analysis on the change generated by the imposition of over-pressure, the calculated temperature was matched with the measured data at the beginning stage of the test-irradiation, during which no over-pressurization was performed, by deducting 15 K from the calculated value for the whole test-irradiation period. In the

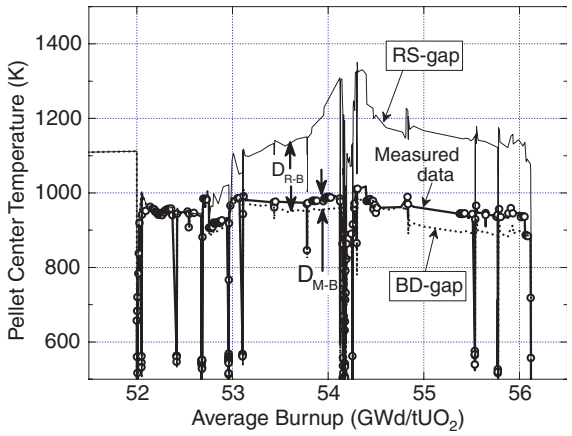

Fig. 7. Comparison of fuel center temperatures. Thick line with open circles is the measured data. Calculated results are given by the two models; bonding gap model (BD-gap) and Ross–Stoute model (RS-gap).

figure, the fuel center temperature is higher than the measurement by 100–300 K during the gap opening period.

(2) BD-gap Case result (broken curve): Similarly to the RS-gap case curve, the value after 15 K deduction from the calculation for the whole test period with **BDC** is shown by the thick curve. The calculation is much closer to the measurement than in the RS-gap case.

4. Discussion

4.1. Center temperature rise

It is evident from the comparison of Figs. 4 and 5 with Fig. 7 that, during the 'gap re-opening' period indicated in Fig. 5, the measured center temperature appreciably exceeds the BD-gap case prediction (BDg), so that it is strongly suggested that the cladding diameter increase shown in Fig. 4 gives rise to some decrease in thermal conductance inside the fuel rod. However, this measured temperature rise is too small in comparison with the rise by the RS-gap case prediction (RSg). The latter is an expected rise of temperature produced by the pellet-clad gap re-opening shown in Fig. 5 where a numerical gap size increases up to a few tens of μm in the RS-gap case.

Here, these temperature differences are analyzed. First, two types of difference of the curves are defined: $D_{\text{R-B}}$, which is obtained by deducting the BDg from RSg, and $D_{\text{M-B}}$, obtained by deducting the BDg from the measured data. In the former period, or from 53.2 GW d/t to 54.1 GW d/t, $D_{\text{R-B}}$ ranges from 100 K (at 52.8 GW d/t) to 330 K (54.3–54.4 GW d/t), while $D_{\text{M-B}}$ is limited to 10–40 K. Assuming that the temperature rise of $D_{\text{M-B}}$ is generated by some 'thermal resistance' which takes place in the inner region of pellet, such as a circumferential thin crack, radial location of the resistance is estimated as follows.

It is noted that the heat flux at the pellet radial location R is defined as the heat generation by the unit length volume of pellet from center (or center-hole wall) to the radius R divided by surface area $2\pi R$. Also, an approximation is assumed that the temperature jump across the gap or crack is proportional to the heat flux passing the gap or crack, or next relationship holds.

$$[\text{Heat flux}] \propto \left[\frac{\text{Volume}}{\text{Radius}}\right] \propto [\text{Temperature jump}]. \quad (4)$$

Then, to obtain the relative heat flux at R, relative heat generations at the ten radial ring elements are compared in Fig. 3, where the relative generation increases linearly with radius in the inner 1- to 9th ring elements due to a flat profile of the heat generation density, and the outermost 10th ring element occupies about 26% of the total heat generation.

Here, $D_{\text{M-B}}$ is much smaller than $D_{\text{R-B}}$, suggesting that the thermal resistance takes place by over-pressure at sufficiently inner element other than the 10th ring element. To estimate the radial location of this thermal resistance, the next calculation is made.

$D_{\text{R-B}}$ is a temperature jump that is generated by the total heat flux, because it is expected to occur at the proper pellet-clad gas gap. Therefore, if the thermal resistance took place at the boundary dividing the 10th and 9th rings, the temperature jump would be 74% or less of the $D_{\text{R-B}}$, because temperature of Argon at the boundary increases by a few tens of Kelvin, so that the thermal conductivity of the gas rises by a few percents according to the equation [11]:

$$k = 3.421 \times 10^{-4} T^{0.701} \ (\text{W/mK}). \quad (5)$$

Assuming that the pellet outer surface is at 650 K and the center is at 1000 K at most, the ratio of thermal conductivity of Argon, or the variation factor of thermal conductance of the resistance is by Eq. (5),

$$[k(1000\ \text{K})/k(650\ \text{K})] = 1.36. \quad (6)$$

This implies that if the thermal resisitance (gap) is located at the vicinity of fuel center, the gap gas conductance would be 36% larger than at the boundary between the 9th and 10th rings. Therefore, if the thermal resistance occurs at the radial position x which is located in between the 9th ring (not the 10th ring) and the center-hole wall of 1.15 mm radius, x will lie in between the values determined by the two equations:

$$\frac{4.56^2 - 1.15^2}{4.56} \times D_{\text{M-B}} = \frac{x^2 - 1.15^2}{x} \times (D_{\text{R-B}} \times 0.74), \quad (7)$$

$$\frac{4.56^2 - 1.15^2}{4.56} \times D_{\text{M-B}} = \frac{x^2 - 1.15^2}{x} \times (D_{\text{R-B}} \times 0.544). \tag{8}$$

Here, 0.544 = 0.74/1.36.

Substituting $D_{\text{R-B}} = 110$ (or 330) and $D_{\text{M-B}} = 10$ (or 20) into Eqs. (7) and (8) gives $x = 1.24$–2.17 mm, suggesting that the 'thermal resistance' occurs 0.09–1.02 mm distant from the wall of the center-hole of 1.15 mm radius, i.e. at the inner region with relative radial position of 27–48%. However, inner region of fuel has high temperature, and thermal stress is compressive or substantially relieved, so that it is quite unlikely that the over-pressurization has generated a circumferential crack. Consequently, it can be appropriate to attribute the temperature rise in the former period to the effective decrease in thermal conductance due to the following mechanism: bonding layer is not broken and pellet fragment moves with cladding creep-out, thus irregular relocation of pellet fragments occurs or fine fission gas pores are generated under relaxation of compressive stress.

In the latter period, from 54.3 GW d/t to 56.1 GW d/t, a similar calculation is conducted by substituting $D_{\text{R-B}} = 240$ and $D_{\text{M-B}} = 60$:

$$\frac{4.56^2 - 1.15^2}{4.56} \times 60 = \frac{x^2 - 1.15^2}{x} \times (240 \times 0.74), \tag{9}$$

$$\frac{4.56^2 - 1.15^2}{4.56} \times 60 = \frac{x^2 - 1.15^2}{x} \times (240 \times 0.544). \tag{10}$$

Solving this equation gives $x = 2.08$–2.49 mm, indicating that the thermal resistance occurs 0.93–1.34 mm distant from the center-hole wall, i.e. at the inner region with relative radial position of 46–55%. Similarly to the former period analysis, the temperature rise is attributable to the effective decrease in conductance rather than substantial circumferential cracking while bonding layer remains unbroken. However, it should be taken into consideration that the thermal conductance decrease in the latter period is capable of being promoted by a number of rapid transients or thermal cycles that the rod experienced during 54.2–54.3 GW d/t.

That the bonding layer was not broken is also suggested by the experimental observation of cladding axial elongation exceeding the thermal expansion of cladding itself to a significant extent [1].

4.2. Evaluation of the experiment

The measured center temperature rise $D_{\text{M-B}}$ is much lower than the hypothetical rise $D_{\text{R-B}}$ that would be caused by the gap re-opening. However, the $D_{\text{M-B}}$ in Fig. 7 is clearly associated with the calculated creep-out of cladding shown in Fig. 5. This analytical result reveals that the over-pressure of ~20 MPa during the former period made the cladding creep outward in excess of expansion and swelling of pellet and that this cladding creep-out was maintained by the over-pressure of ~12 MPa in the latter period. This is consistent with Beguin's deduction that the threshold over-pressure is around 15 MPa in the experiment [1], and the present analyses validated the method in the IFA-610.1 test in which fuel center temperature rise was associated with over-pressure as an indicator of the Lift-Off.

5. Conclusion

Experimental analysis was conducted by the fuel performance code FEMAXI-6 on the Lift-Off experiment in Halden reactor, and validated the method of the experiment. The most important result is that the measured center temperature is higher by a few tens of K than the prediction assuming an enhanced thermal conductance across the pellet-clad bonding layer. However, this difference is much smaller than the calculated temperature rise assuming the gap re-opening generated by cladding creep-out. Therefore, it is appropriate to attribute the observed rise to the decrease in effective thermal conductance due to irregular re-location of pellet fragments, etc. It can be seen also from the calculation that the bonding layer is not broken by the over-pressure and keeps an enhanced pellet-clad thermal conductance even during the cladding creep-out process.

Acknowledgments

The authors thank Dr S. Beguin of EdF for his early supervision and evaluation of the IFA-610.1 experiment, Halden Reactor Project for provision of useful information in TFDB, and Dr W. Wiesenack of Halden Reactor Project for his kind instructions for the publication of the present analysis.

References

[1] S. Beguin, HWR-544, 1998.
[2] M. Suzuki, H. Uetsuka, H. Saitou, Nucl. Eng. Des. 229 (2004) 1.
[3] M. Suzuki, JAERI Data/Code 2000-030, 2000.
[4] M. Suzuki, Nucl. Eng. Des. 201 (2000) 99.
[5] W. Wiesenack, M. Vankeerberghen, R. Thankappan, HWR-469, 1996.
[6] D. Schrire, A. Kindlund, P. Ekberg, HPR-349/22, 1998.
[7] D.L. Hagrman, G.A. Reyman, MATPRO-Version11, NUREG/CR-0497, TREE-1280, Rev. 3, 1979.
[8] A.M. Ross, R.L. Stoute, CRFD-1075, 1962, p. 970.
[9] M.A. McGrath, in: Proceedings of the 2000 International Topical Meeting on LWR Fuel Performance, Park City, USA, 2000.

[10] K. Une, K. Nogita, S. Kashibe, T. Toyonaga, M. Amaya, in: Proceedings of the International Topical Meeting on LWR Fuel Performance, Portland, USA, 1997, p. 478.
[11] MATPRO-A, NUREG/CR-6150, 1995.
[12] W. Wiesenack, V. Hustadnes, HWR-338, 1993.
[13] M. Uchida, H. Saitou, JAERI-M 93-108, 1993 (in Japanese).